

Modeling Continuous Motion for 3D Point Cloud Object Tracking

Zhipeng Luo^{1,2} Gongjie Zhang¹ Changqing Zhou² Zhonghua Wu²
 Qingyi Tao² Lewei Lu² Shijian Lu^{1*}
¹ Nanyang Technological University ² SenseTime Research

Abstract

The task of 3D single object tracking (SOT) with LiDAR point clouds is crucial for various applications, such as autonomous driving and robotics. However, existing approaches have primarily relied on appearance matching or motion modeling within only two successive frames, thereby overlooking the long-range continuous motion property of objects in 3D space. To address this issue, this paper presents a novel approach that views each tracklet as a continuous stream: at each timestamp, only the current frame is fed into the network to interact with multi-frame historical features stored in a memory bank, enabling efficient exploitation of sequential information. To achieve effective cross-frame message passing, a hybrid attention mechanism is designed to account for both long-range relation modeling and local geometric feature extraction. Furthermore, to enhance the utilization of multi-frame features for robust tracking, a contrastive sequence enhancement strategy is designed, which uses ground truth tracklets to augment training sequences and promote discrimination against false positives in a contrastive manner. Extensive experiments demonstrate that the proposed method outperforms the state-of-the-art method by significant margins (approximately 8%, 6%, and 12% improvements in the success performance on KITTI, nuScenes, and Waymo, respectively). Codes will be made publicly available.

1. Introduction

The rapid advancement of LiDAR technology has sparked a growing interest in point cloud-based vision solutions over recent years. 3D single object tracking (SOT) based on point clouds is a fundamental task that holds enormous potential for various applications, including autonomous driving and robotics. Nevertheless, 3D SOT remains a challenging and open problem owing to the inherent nature of point clouds. Factors such as point sparsity, partial observation, and lack of texture information make this task

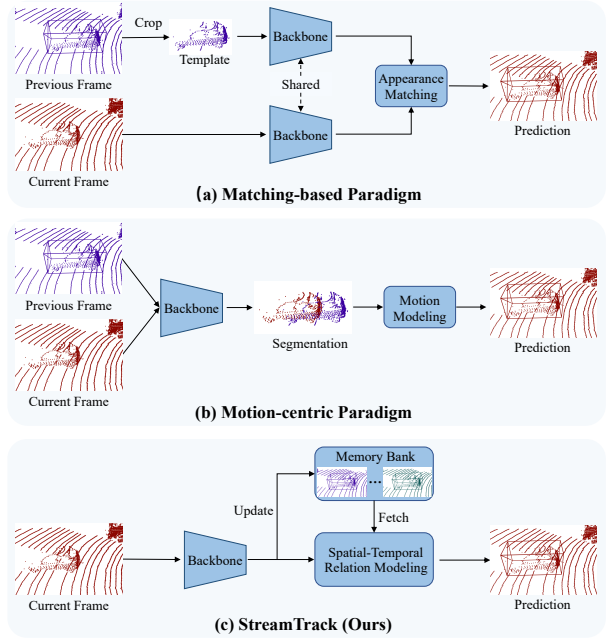


Figure 1. Comparison of 3D single object tracking paradigms. (a) The matching-based paradigm extracts features from a cropped template and a search region, and object localization is performed based on appearance matching. (b) The motion-centric paradigm takes concatenated point cloud frames as input and estimates relative motion based on segmented objects. (c) Our proposed StreamTrack only uses the current frame as input, while historical features are fetched from a memory bank, allowing for the exploitation of multi-frame continuous motion for robust tracking.

particularly difficult to solve. The development of effective 3D SOT solutions continues to be an active research focus.

Most existing 3D SOT approaches, such as [10, 28, 6, 37, 42, 16, 44, 17, 13], follow the prevalent paradigm of appearance matching (Fig. 1(a)), which originated from their 2D counterparts [33, 12, 1, 20, 21]. Such matching-based methods perform feature matching between a cropped template and a search region to locate target objects but are prone to errors in cases of fast movement, occlusion, and misleading objects with similar appearances. Recently, a new motion-centric paradigm [43] (Fig. 1(b)) has been pro-

*Corresponding author

posed for 3D SOT, which uses concatenated point clouds from two successive frames as input to preserve the motion connection. It performs motion estimation based on segmented foreground points to predict the relative motion and achieves outstanding tracking performance. However, it has two limitations. First, it neglects the dynamics (*e.g.*, velocity and acceleration) contained in multi-frame historical movements, which could provide strong cues to future motion. Second, the segmentation stage eliminates background points, which might contain helpful contextual information for subsequent object localization. Erroneous segmentation could also affect tracking adversely.

Based on the aforementioned observations, we aim to propose a solution that can effectively exploit multi-frame continuous motion for accurate and robust object tracking. A naive method would be to extend the existing motion-centric paradigm by concatenating points from multiple frames to form the input. However, this approach would result in increased computational overhead and a potential problem that objects could exceed the predefined search range. To address these issues, we propose a new framework for 3D SOT named *StreamTrack*. As shown in Fig. 1(c), in this paradigm, each tracking sequence is treated as a *stream*: at each timestamp, only the current frame is used as input, while historical features are stored in a live memory bank. Multi-frame features undergo a spatial-temporal relation modeling process to generate tracking predictions in an end-to-end manner. To achieve effective cross-frame message passing, we design a hybrid attention mechanism that can handle both long-range relation modeling and local geometric feature extraction simultaneously. To further improve the utilization of multi-frame features for robust tracking, we incorporate a contrastive sequence enhancement strategy where ground truth tracklets are used to augment training sequences and promote discrimination against false positives in a contrastive manner. This effectively mitigates the issue of target-switch, where a wrong object is tracked during tracking. We evaluate our proposed approach on KITTI, nuScenes, and Waymo datasets, and the experimental results demonstrate that *StreamTrack* achieves new state-of-the-art performance on all benchmarks.

The contributions of this work are summarized below: **1)** We identify an overlooked aspect in existing 3D SOT paradigms and propose *StreamTrack* – a new paradigm that treats each tracking sequence as a stream and utilizes a memory bank for efficient exploitation of multi-frame continuous motion; **2)** We propose a hybrid attention mechanism that can handle both long-range relation modeling and local geometric feature extraction to achieve effective cross-frame message passing; **3)** We design a contrastive sequence enhancement scheme that further improves the utilization of multi-frame features for robust tracking; **4)** Experimental results on KITTI, nuScenes, and Waymo demon-

strate that *StreamTrack* achieves new state-of-the-art performance while still being computationally efficient.

2. Related Work

3D Single Object Tracking. Given a point cloud sequence and the bounding box of an object in the first frame, the goal of 3D SOT is to locate the object in subsequent frames. Most existing 3D SOT approaches follow two paradigms, namely matching-based paradigm and motion-centric paradigm. Specifically, a number of methods follow the matching-based paradigm, which is inspired by the success of Siamese networks in 2D SOT [33, 1, 21, 20, 12]. As the pioneering work, SC3D [10] generates a series of target proposals to match with the template based on feature similarities and selects the proposal with the top similarity as the prediction. However, the heuristic proposal sampling process is time-consuming and does not allow end-to-end training. P2B [28] uses a Region Proposal Network [26] for efficient proposal generation and employs Hough Voting to generate the tracking prediction. Motivated by the success of P2B, a series of follow-up work further improves the feature correlation operation or prediction generation with more sophisticated designs. For example, SA-P2B [45] designs an auxiliary task to learn the structure of objects. BAT [42] encodes structural information with Box Cloud for individual points. MLVSNet [37] enhances the feature aggregation with multi-level Hough Voting. V2B [16] performs Voxel-to-BEV transformation for object localization on the densified feature maps.

Inspired by the outstanding performance of Transformer [35] on various computer vision tasks [7, 24, 3], several studies [44, 6, 30, 17, 13] incorporate Transformer for enhanced feature extraction and correlation modeling. We also adopt Transformer to perform spatial-temporal relation modeling to leverage its strong capacity for learning long-range dependencies. Differently, we propose a hybrid attention mechanism to enhance local geometric feature extraction for more effective cross-frame message passing. As far as we know, this is the first work that incorporates local attention for feature extraction in the 3D SOT family.

Despite its success, the matching-based paradigm breaks the motion connection between successive frames with template cropping and does not fully exploit the distortion-free property of point clouds. This makes it sensitive to distractors with similar geometric shapes [43]. Recently, a motion-centric tracker M²-Track [43] achieves superb tracking performance by tackling the tracking problem from the perspective of relative motion. Our proposed method is more related to the motion-centric paradigm but differs from M²-Track by exploiting multi-frame continuous motion and having an end-to-end design.

Contrastive Learning works under the principle that similar sample pairs should be close in a learned embed-

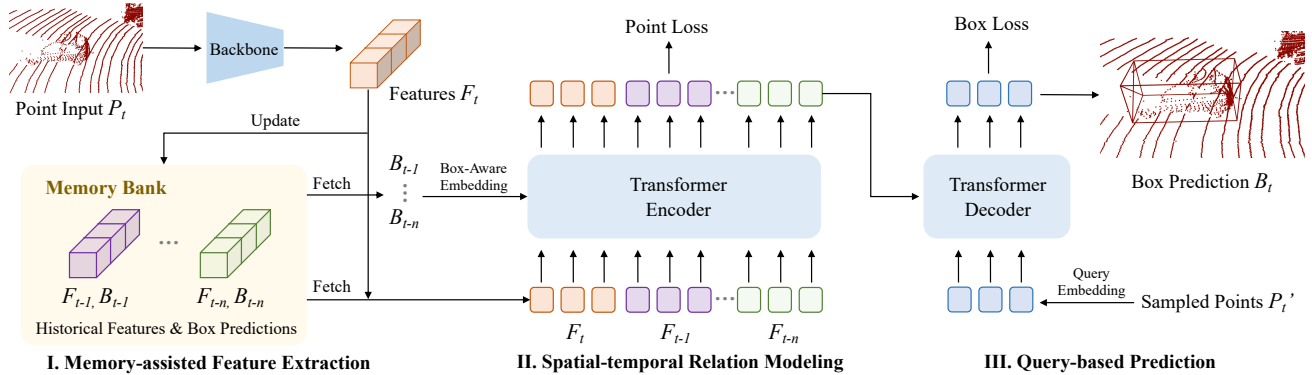


Figure 2. Overall architecture of StreamTrack. StreamTrack consists of three parts: memory-assisted feature extraction, spatial-temporal relation modeling, and query-based prediction. At each timestamp t , StreamTrack only takes as input the current frame P_t , while historical features and box predictions are fetched from a memory bank for efficient computation. A Transformer encoder-decoder architecture is adopted for the message passing among multi-frame features and the generation of tracking predictions in an end-to-end manner.

ding space, while distinct ones should be well separated. It has been extensively studied in representation learning [5, 14, 15, 25, 39, 11] and achieved remarkable success in boosting the performance of downstream tasks. Several studies [19, 38, 46, 40] extend contrastive learning to the supervised setting to learn more robust feature representations to reduce misclassification or wrong instance associations. Inspired by the above work, we design a contrastive sequence enhancement strategy to improve the robustness of tracking. To our best knowledge, this is the first effort to utilize contrastive learning in 3D SOT approaches.

3. Methodology

As illustrated in Fig. 2, our proposed StreamTrack consists of three modules: 1) memory-assisted feature extraction (Sec. 3.1), 2) spatial-temporal relation modeling (Sec. 3.2), and 3) query-based prediction (Sec. 3.3). We describe them in detail in the remainder of this section.

3.1. Memory-assisted Feature Extraction

Existing 3D SOT methods following either the matching-based or motion-centric paradigm typically rely on point clouds from two consecutive frames as input. However, multiple frames capture richer motion information, which can be exploited for more accurate and robust tracking. One possible approach to utilize multi-frame information is to concatenate points from a number of frames to form the input as in [43]. However, such an approach becomes computationally expensive as the number of points increases. Additionally, fast-moving objects may go beyond the predefined search range, as a small range is typically used to reduce search complexity and improve efficiency.

To address these issues, we propose a memory-assisted feature extraction scheme for the efficient utilization of multi-frame features. As shown in Fig. 2, given a point

cloud frame $P_t \in \mathbb{R}^{N \times 3}$ at timestamp t , where N is the number of input points, we use a backbone model to extract the point features $F_t \in \mathbb{R}^{N' \times C}$, where N' is the number of points sampled by the backbone and C is channel dimension. We adopt PointNet++ [27] as our backbone as it is adopted in many existing 3D SOT methods [28, 42, 44], although it is possible to use more sophisticated backbone networks to further improve the tracking performance. We employ a memory bank to store historical point features and box predictions of the past n frames, which are denoted by $\{F_{t-i}\}_{i=1}^n$ and $\{B_{t-i}\}_{i=1}^n$, respectively. At the end of each iteration, we update the memory bank with F_t and B_t and discard those from the earliest frame (F_{t-n} and B_{t-n}).

The memory bank design allows us to bypass the repetitive computation of multi-frame point features and greatly improves the efficiency of our framework. One major difference between the input of M²-Track and our StreamTrack is that M²-Track uses a unified coordinate system for the two successive frames at each timestamp, whereas we shift the coordinate system for each frame to follow the movement of objects. Specifically, the canonical coordinate system defined by B_{t-1} is employed for input P_t . This design allows reusing historical features without enlarging the input range to cover long-range movements.

3.2. Spatial-temporal Relation Modeling

The goal of this module is to model the cross-frame relation and propagate target information from past frames to the current frame for subsequent object localization. To deal with the complexity introduced by multi-frame features, we employ the attention mechanism of Transformer [35] to leverage its strong capability to model long-range dependencies. Specifically, we use an encoder consisting of L_{enc} stacked Transformer layers to encode point features and historical box locations. In the following text, we first describe the spatial-temporal relation modeling process us-

ing the original (vanilla) attention mechanism [35] and then introduce our proposed hybrid attention designed for more effective cross-frame feature exchange.

Vanilla Attention. For each Transformer layer, given point features $\{F_t, F_{t-1}, \dots, F_{t-n}\}$, we first concatenate them to form the input $F \in \mathbb{R}^{(n+1) \times N' \times C}$. Since the attention mechanism of Transformer treats the features of each point as individual tokens without including the relative positions of the points, we generate a position embedding PE , which is of the same shape as F , by mapping the xyz coordinates of the points with an MLP. To distinguish points from different frames, we also add a learnable temporal embedding to PE based on the temporal sequential order. Besides, the tracking process is conditioned on the prior knowledge of object locations in past frames. To incorporate past box locations, we generate a point mask $M \in \mathbb{R}^{(n+1) \times N'}$ to indicate the objectiveness of each point as in [43]. Concretely, $m_j^i \in M$ is defined as:

$$m_j^i = \begin{cases} 0 & \text{if } j \in [t-1, t-n] \text{ and } p_j^i \text{ is not in } B_j \\ 1 & \text{if } j \in [t-1, t-n] \text{ and } p_j^i \text{ is in } B_j \\ 0.5 & \text{if } j = t \end{cases} \quad (1)$$

where i indexes the points and j indexes the timestamps. Intuitively, m_j^i can be viewed as the probability of point p_j^i belonging to the foreground, and other arbitrary values can be used for the same purpose of indicating objectiveness. However, M does not accurately encode the box location and orientation especially when points are sparse. [42] proposes to represent the point-to-box relation by including the distances from each point to the box center and 8 corners. We concatenate the said distances to M and obtain the box-aware point mask $M' \in \mathbb{R}^{(n+1) \times N' \times (1+9)}$, where the distance values for the current frame are set to zero due to unknown box location. Similarly, we map M' with an MLP to obtain a box-aware mask embedding ME . Finally, we add the position embedding to F to form query and key, while adding the mask embedding to F to obtain value, and perform the attention computation as defined in [35]:

$$Q = K = F + PE; \quad V = F + ME \quad (2)$$

$$F' = \text{Softmax}\left(\frac{QK^T}{\sqrt{d_k}}\right)V \quad (3)$$

where F' denotes the attention output and d_k is the key dimension. A standard feedforward network (FFN) is further applied to generate the output of the Transformer layer.

Hybrid Attention. Albeit the strong global relation modeling capability of Transformer, it treats each point equally without paying specific attention to local geometric structures, which have been proven to be crucial in various point representation learning studies [27, 36, 34, 41]. To achieve more effective cross-frame message passing, we design a

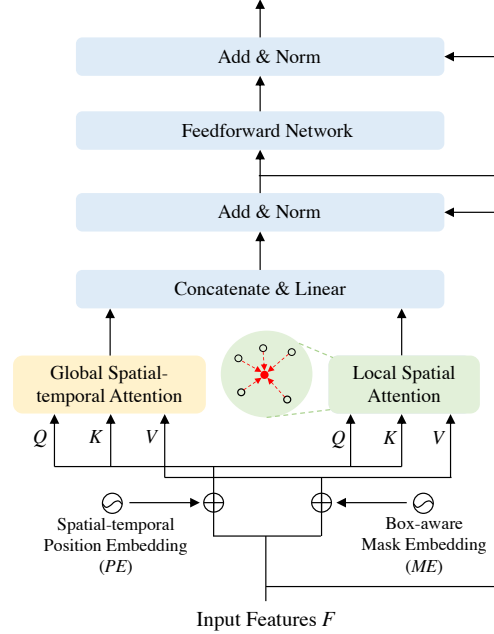


Figure 3. Architecture of the proposed hybrid attention. A local spatial attention module is introduced to work in parallel with global spatial-temporal attention to account for both local feature extraction and long-term relation modeling to achieve more effective cross-frame message passing.

hybrid attention mechanism that incorporates such inductive bias into Transformer. As shown in Fig. 3, we introduce a local spatial attention operation in parallel with the regular global temporal attention to account for both local geometric feature extraction and long-range relation modeling. Specifically, we gather a local set of points $\{p_b | |p_b - p_a| < r\}$ for each input point p_a with a pre-defined distance threshold r and replace K and V in the vanilla attention with the corresponding local point features. The outputs of both attention modules are then concatenated and merged with a Linear layer. The proposed hybrid attention enhances the learning of local geometric structures to improve the modeling of spatial-temporal relations.

Point Supervision. To promote cross-frame feature interaction and information propagation, we apply point-wise supervision on the output of the encoder. Specifically, for each encoder layer, we predict a segmentation mask s and a distance mask d as defined in the previous box-aware point mask generation. The point loss \mathcal{L}_{point} is formulated as:

$$\mathcal{L}_{point} = \sum_l^{L_{enc}} (\lambda_s \mathcal{L}_{CE}(s_l, \hat{s}) + \lambda_d \mathcal{L}_{smooth-l1}(d_l, \hat{d})) \quad (4)$$

where $\hat{(\cdot)}$ denotes the ground truth, l indexes the encoder layers, and \mathcal{L}_{CE} represents the cross-entropy loss.

3.3. Query-based Prediction

Most existing 3D SOT methods [28, 42, 44, 13, 17] employ point-based RPNs to generate tracking predictions. Inspired by the prevalent DETR [4] detection paradigm, we introduce a query-based prediction method in this work. As shown in Fig. 2, we first generate query embeddings based on the coordinates of the sampled points P'_t using an MLP. The query embeddings are then input to a decoder consisting of L_{dec} Transformer layers to interact with the encoder output for tracking prediction generation. Each decoder layer contains a self-attention followed by a cross-attention as described in [4]. Unlike RPN-based approaches, which generate tracking predictions over the current frame, our approach allows each object query to interact with encoded features from all frames, leveraging the attention mechanism of Transformer.

Box Supervision. For each decoder layer, a classification head and a regression head are applied to generate class predictions c in the form of probability and box predictions b . We then perform box matching to match the predictions to the ground truth bounding box \hat{b} . The matching process is similar to the set-to-set matching in [4] except that we aim to find one single prediction that is best matched to the ground truth. We define the matching cost function with a semantic term and a geometric term:

$$\mathcal{L}_{match} = -\lambda_{cls}c - \lambda_{giou}\mathcal{L}_{giou}(b, \hat{b}) \quad (5)$$

where \mathcal{L}_{giou} measures the box overlap using GIoU [29]. We then select the prediction with the lowest matching cost as the positive prediction and set the classification target as one, while the rest are regarded as negative predictions with classification targets of zeros. Finally, the box loss can be formulated by:

$$\mathcal{L}_{box} = \sum_l^{L_{dec}} (\lambda_{cls}\mathcal{L}_{focal}(c_l, \hat{c}_l) + \lambda_{reg}\mathcal{L}_{reg}(b_l^+, \hat{b})) \quad (6)$$

where \mathcal{L}_{focal} denotes the focal loss [23], and the regression loss \mathcal{L}_{reg} consists of smooth-L1 and GIoU terms, which is detailed in the Appendix. Note that the regression loss is only applied to the best-matched positive prediction b_l^+ .

Contrastive Sequence Enhancement. It has been identified in prior work [43] that distractors (nearby objects with similar appearances) pose a significant challenge to 3D SOT as point clouds provide limited appearance cues due to their textureless nature. We observe that there might not exist an abundance of distractors in the training sequences since typically only a small search region is considered, especially under data-constrained scenarios. As a result, tracking methods may not be fully trained to discriminate against negative targets. To this end, we propose a *sequence enhancement* scheme by purposely attaching additional tracklets to training sequences to serve as negative samples. As

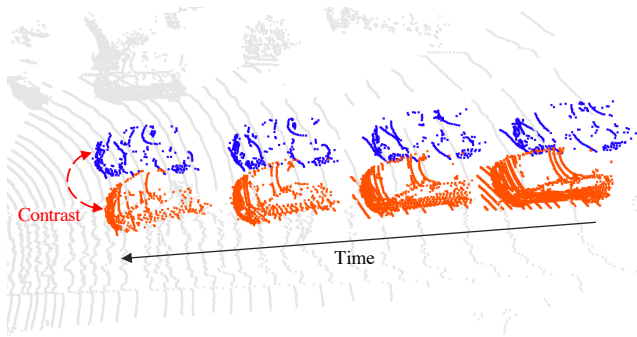


Figure 4. Illustration of contrastive sequence enhancement. Blue points denote the original target object in a tracking sequence, and orange points represent the added tracklet which serves as a negative sample. An auxiliary contrastive loss is applied to further promote discrimination against false positives.

illustrated in Fig. 4, with a probability of ρ , we randomly sample a tracklet of the same length as the training input frames from the training data and attach it to the input. The added objects are placed near the target object with a randomly generated relative velocity to simulate object movements. Note that although the proposed sequence enhancement shares some similarities with the commonly used ‘GT-AUG’ [31] on the 3D detection task, they differ in the following aspects. First, ‘GT-AUG’ is usually applied to a single frame, while sequence enhancement works with sequential frames. Second, ‘GT-AUG’ introduces additional positive targets, whereas sequence enhancement attaches negative samples to enhance discrimination.

Motivated by the success of contrastive learning [5, 14, 15], we introduce an auxiliary contrastive loss to explicitly enforce the separation between positive and negative targets in the feature embedding space. Specifically, we add an additional GT query as in [22] by generating its query embedding based on the center location of the ground truth bounding box. Note that the inclusion of the GT query does not have a significant impact on the tracking performance (see Appendix). The prediction generated by the GT query naturally forms a positive pair with the best-matched positive prediction and forms negative pairs with the remaining negative predictions. We follow the practice in MoCo [14] to generate GT feature embedding f_g with a momentum decoder obtained via exponential moving average, and the prediction embeddings are generated by projecting the decoder outputs with an MLP. The auxiliary contrastive loss is calculated using the InfoNCE [25] loss over all decoder layers:

$$\mathcal{L}_{aux} = \sum_l^{L_{dec}} -\log \frac{\exp(f_g^l \cdot f_+^l / \tau)}{\sum_{i=1}^{N'} \exp(f_g^l \cdot f_i^l / \tau)} \quad (7)$$

where f_+^l denotes the feature embedding of the matched positive prediction, and τ is a temperature hyper-parameter

defined in [39]. Note that contrastive sequence enhancement is only applied during training so that it brings no extra computation to the inference process.

3.4. Implementation Details

Loss Function. We define the total loss function as the linear sum of the point loss, the box loss, and the auxiliary contrastive loss:

$$\mathcal{L}_{total} = \lambda_{point}\mathcal{L}_{point} + \lambda_{box}\mathcal{L}_{box} + \lambda_{aux}\mathcal{L}_{aux} \quad (8)$$

We include more details such as hyper-parameter values in the Appendix due to space constraints.

Training and Inference. During training, we randomly sample $n + 1$ consecutive frames from a tracking sequence to form a training sample, and the point features of all frames are extracted by the backbone network on the fly. During inference, we store historical features and box predictions in the memory bank for efficient computation.

Data Augmentation. Similar to M²-Track [43], we apply box augmentation and motion augmentation to the input data during training. For box augmentation, we follow existing methods [28, 42, 44, 43] to add a small random shift to bounding boxes on historical frames to simulate prediction errors during inference. For motion augmentation, M²-Track employs object-wise augmentation by randomly transforming bounding boxes together with the points inside to diversify the relative motion. We instead perform frame-wise augmentation as in matching-based methods [28, 42, 44] by transforming all points from individual frames since our prediction process is based on global point features rather than only foreground points as in M²-Track.

4. Experiments

4.1. Experiment Setups

Datasets. We conduct extensive evaluations on three widely used datasets: KITTI [9], nuScene [2], and Waymo Open Dataset [32]. The KITTI dataset contains 21 training sequences and 29 testing sequences, and we follow the data split defined in prior studies [28, 10, 42]. The nuScenes and Waymo datasets are of significantly larger scales as compared to KITTI. We follow the implementation of [43] for these two datasets, except we randomly sample 10% of the tracklets for training on the Waymo dataset due to its overwhelming sample size. Testing is conducted over all test samples to ensure fair comparisons. Note that the nuScenes and Waymo datasets are more challenging than KITTI due to their category diversity and scene complexity. In particular, both KITTI and Waymo have a frame rate of 10Hz, while nuScenes only provides annotations at 2Hz although it has a frame rate of 20Hz. Since only annotated frames are used for training, it poses extra difficulties to trackers.

Category		Car	Pedestrian	Van	Cyclist	Mean
Number of Frames		6424	6088	1248	308	14068
Success	SC3D [10]	41.3	18.2	40.4	41.5	31.2
	P2B [28]	56.2	28.7	40.8	32.1	42.4
	MLVSNet [37]	56.0	34.1	52.0	34.3	45.7
	3D-SiamRPN [8]	58.2	35.2	45.6	36.1	46.6
	SA-P2B [45]	58.0	34.6	51.2	32.0	46.7
	LTTR [6]	65.0	33.2	35.8	66.2	48.7
	BAT [42]	65.4	45.7	52.4	33.7	55.0
	PTT [30]	67.8	44.9	43.6	37.2	55.1
	PTTR [44]	65.2	50.9	52.5	65.1	57.9
	V2B [16]	70.5	48.3	50.1	40.8	58.4
	CMT [13]	70.5	49.1	54.1	55.1	59.4
	STNet [17]	72.1	49.9	58.0	73.5	61.3
	M ² -Track [43]	65.5	61.5	53.8	73.2	62.9
	StreamTrack(Ours)	72.6	70.5	61.0	78.1	70.8
Precision	SC3D [10]	57.9	37.8	47.0	70.4	48.5
	P2B [28]	72.8	49.6	48.4	44.7	60.0
	MLVSNet [37]	74.0	61.1	61.4	44.5	66.7
	3D-SiamRPN [8]	76.2	56.2	52.8	49.0	64.9
	SA-P2B [45]	75.1	63.3	63.1	43.6	68.2
	LTTR [6]	77.1	56.8	45.6	89.9	65.8
	BAT [42]	78.9	74.5	67.0	45.4	75.2
	PTT [30]	81.8	72.0	52.5	47.3	74.2
	PTTR [44]	77.4	81.6	61.8	90.5	78.1
	V2B [16]	81.3	73.5	58.0	49.7	75.2
	CMT [13]	81.9	75.5	64.1	82.4	77.6
	STNet [17]	84.0	77.2	70.6	93.7	80.1
	M ² -Track [43]	80.8	88.2	70.7	93.5	83.4
	StreamTrack (Ours)	83.7	94.7	76.9	94.6	88.1

Table 1. Performance comparison on the KITTI dataset. *Mean* performance is weighted by the number of frames.

Evaluation Metrics. We follow existing studies [10, 28, 42] and use the One Pass Evaluation [18] to measure the *Success* and *Precision* of tracking predictions. *Success* is computed from the intersection over union (IOU) of the predicted bounding box and the ground truth box, while *Precision* is defined as the area under the curve (AUC) for the distance between two box centers from 0 to 2 meters.

4.2. Benchmarking Results

Results on KITTI. As shown in Tab. 1, the proposed StreamTrack outperforms existing methods on most categories and surpasses the state-of-the-art method M²-Track [43] by large margins of 7.9% and 4.7% in average success and average precision, respectively. Notably, matching-based methods (*e.g.*, STNet [17] and CMT [13]) tend to perform well on Car and Van, while motion-centric method M²-Track is competitive on Pedestrian and Cyclist. We conjecture that cars and vans are rigid in shape and relatively sizeable, which makes them suitable for appearance matching. In contrast, humans are non-rigid and often appear in crowds, which poses challenges to the matching process. On the other hand, although M²-Track is more robust to distractors due to its motion-centric property, its use of simple operations (*e.g.*, MLP and max-pooling) for feature extraction limits the capability of learning geometric structures.

	Dataset Category	nuScene					Mean	Waymo [‡]		
		Car	Pedestrian	Truck	Trailer	Bus		Vehicle	Pedestrian	Mean
Number of Frames		64,159	33,227	13,587	3,352	2,953	117,278	1,057,651	510,533	1,568,184
Success	SC3D [10]	22.31	11.29	30.67	35.28	29.35	20.70	-	-	-
	P2B [28]	38.81	28.39	42.95	48.96	32.95	36.48	28.32	15.60	24.18
	BAT [42]	40.73	28.83	45.34	52.59	35.44	38.10	35.62	22.05	31.20
	M ² -Track [43]	55.85	32.10	57.36	57.61	51.39	49.23	43.62	42.10	43.13
	StreamTrack (Ours)	62.05	38.43	64.67	66.67	60.66	55.75	60.23	47.07	55.95
Precision	SC3D [10]	21.93	12.65	27.73	28.12	24.08	20.20	-	-	-
	P2B [28]	42.18	52.24	41.59	40.05	27.41	45.08	35.41	29.56	33.51
	BAT [42]	43.29	53.32	42.58	44.89	28.01	45.71	44.15	36.79	41.75
	M ² -Track [43]	65.09	60.92	59.54	58.26	51.44	62.73	61.64	67.31	63.48
	StreamTrack (Ours)	70.81	68.58	66.60	64.27	59.74	69.22	72.61	70.44	71.90

[‡] On Waymo, StreamTrack only uses 10% randomly sampled tracklets for training, while others use all. All methods are evaluated on the full test set.

Table 2. Performance comparison on the nuScene and Waymo datasets. Mean performance is weighted by the number of frames.

In StreamTrack, we propose hybrid attention for effective geometric feature extraction and leverage multi-frame continuous motion for robust tracking, thus achieving balanced performance for all categories.

Results on nuScenes and Waymo. We compare StreamTrack with methods [10, 28, 42, 43] evaluated under the same setting on nuScenes and Waymo. As shown in Tab. 2, StreamTrack similarly achieves new state-of-the-art performance for all categories and outperforms compared methods by notable margins (*e.g.*, a large success gain of 16.61% for the Vehicle category on Waymo). On the Waymo dataset, despite using only 10% of the training samples, our proposed method still outperforms existing methods trained with the full train set. The nuScenes dataset is known for its low point density as it is collected using 32-beam LiDARs as compared to 64-beam for other datasets, while the Waymo dataset captures complex traffic scenes with numerous objects. The outstanding performance of StreamTrack on both datasets demonstrates its strong capability of tracking objects under challenging scenarios.

4.3. Ablation Study

Effectiveness of multi-frame information. The key motivation of StreamTrack is to exploit multi-frame continuous motion for more informed and robust tracking. We conduct experiments to study the impact on performance when information from different numbers of frames (including n historical frames and the current frame) is used to generate the tracking prediction. For a more comprehensive evaluation, we also extend M²-Track [43] to the multi-frame setting¹ by concatenating points from multiple frames to form its input. As shown in Fig. 5, a significant improvement of 4.8% in success is observed for StreamTrack when the number of frames increases from 2 to 3, and the performance stabilizes when the frame number is further increased. We hypothesize that two historical frames could already provide strong motion cues (*e.g.*, velocity and accel-

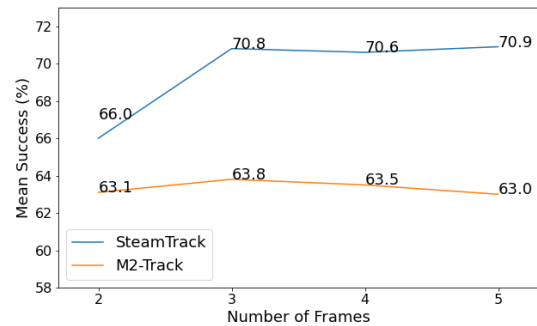


Figure 5. Mean Success vs Number of Frames that are used for predictions, evaluated over the KITTI dataset.

eration) to aid the tracking process, while further increasing the frame count leads to marginal gains and extra complexity. In Fig. 6, we visualize a tracking sequence to further demonstrate the effectiveness of exploiting multi-frame information in improving the robustness of tracking. Based on the experimental results, we use two historical frames ($n = 2$) in our default setting considering the efficiency aspect. On the other hand, the performance of M²-Track only improves marginally when multiple frames are used and a downward trend is observed when the number of frames further increases. This could be attributed to the simple architecture of M²-Track, which is not designed to handle the complex multi-frame feature interaction.

Effectiveness of model components. We conduct comprehensive ablation studies to investigate the effectiveness of the building components of StreamTrack. As shown in Tab. 3, removing hybrid attention (comparing #1 and #7) leads to a decrease of 1.9% in mean success and precision, which validates that the local attention design complements the vanilla global attention mechanism. #2 studies the impact of point supervision, and we observe a notable decrease of 4.9% and 3.4% in mean success and precision compared to our default setting (#7) when the point loss on encoder predictions is removed. In particular, the Pedestrian and Cyclist categories suffer from larger drops, which implies

¹Implemented based on the [official code](#)

#	Hybrid	Point Sup	Query Pred	Seq Enhance	Contrast	Car	Pedestrian	Van	Cyclist	Mean
1		✓	✓	✓	✓	70.5 / 81.2	69.1 / 94.3	57.4 / 70.7	76.5 / 93.4	68.9 / 86.2
2	✓		✓	✓	✓	70.4 / 81.0	62.4 / 90.7	58.7 / 72.3	72.2 / 93.6	65.9 / 84.7
3	✓	✓		✓		70.1 / 81.0	65.1 / 92.3	59.0 / 74.3	75.4 / 94.0	67.1 / 85.6
4	✓	✓	✓			70.1 / 80.6	65.2 / 90.6	52.1 / 63.0	75.1 / 94.3	66.5 / 83.7
5	✓	✓	✓	✓		70.6 / 81.3	67.8 / 93.1	57.4 / 69.0	78.6 / 95.1	68.4 / 85.6
6	✓	✓	✓		✓	70.9 / 81.2	67.6 / 93.5	53.2 / 63.5	77.2 / 94.7	68.0 / 85.2
7	✓	✓	✓	✓	✓	72.6 / 83.7	70.5 / 94.7	61.0 / 76.9	78.1 / 94.6	70.8 / 88.1

Table 3. Ablation studies on model components. ‘Hybrid’ denotes hybrid attention. ‘Point Sup’ denotes point supervision. ‘Query Pred’ denotes our proposed query-based prediction paradigm. When ‘Query Pred’ is disabled, we replace the decoder with the prediction head in [43]. ‘Seq Enhance’ denotes sequence enhancement, and ‘Contrast’ denotes auxiliary contrastive loss. Success / Precision are reported.

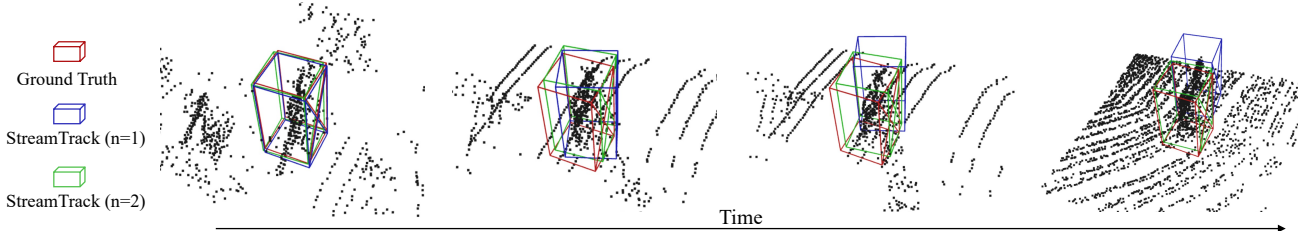


Figure 6. Visualization of tracking predictions on a Pedestrian sequence in which distractors exist. When $n = 1$, StreamTrack only relies on one historical frame, which is similar to the existing motion-centric paradigm [43]. It demonstrates that the exploitation of multi-frame continuous motion improves the tracking robustness effectively.

that low-level supervision is more important for objects of smaller sizes. To investigate the effectiveness of the proposed query-based prediction, we replace the decoder of StreamTrack with the prediction head in [43]. Note that the contrastive loss is dependent on the query-based design so it is not included. By comparing #3 and #5, it can be seen that our query-based prediction achieves improved overall performance, which shows the advantage of utilizing global multi-frame features for prediction generation in our design. From #4 to #7, it can be observed that both sequence enhancement and the auxiliary contrastive loss have a positive impact on the tracking performance. Moreover, they appear to be complementary to each other, as the performance is further improved when both are applied. Remarkably, sequence enhancement introduces a substantial performance improvement (+5.3% in success) to the Van category, which has a limited number of training samples. This shows the potential of the sequence enhancement technique under data-constrained settings.

4.4. Discussion

Inference Speed. Tab. 4 presents the average inference speed, in the form of frame per second (FPS), measured using all test frames from the Car category on the KITTI dataset. We compare our StreamTrack with a number of representative methods, and the speed of all compared methods is measured using the same platform with a single NVIDIA V100 GPU. Thanks to the memory bank design, our proposed StreamTrack achieves a running speed of 40.7 FPS despite the relation modeling based on multi-frame features, which is on par with existing matching-based meth-

Method	FPS	Success	Precision
P2B [28]	38.8	42.4	60.0
BAT [42]	40.9	55.0	75.2
STNet [17]	30.1	61.3	80.1
M ² -Track [43]	54.8	62.9	83.4
StreamTrack(Ours)	40.7	70.8	88.1

Table 4. Inference speed comparison on the KITTI dataset.

ods (e.g., P2B [28] and BAT [42]). Notably, M²-Track [43] is exceptionally fast due to its simple architecture which only consists of pooling operations and MLPs. However, as shown in Fig. 5, such a design is inadequate for the effective exploration of multi-frame information.

Limitations. Our proposed method employs multi-frame information, which results in longer training time due to additional overheads associated with data loading and feature computation. More efficient training schemes could be explored in future research to mitigate this issue.

5. Conclusion

This paper presents StreamTrack, a new framework for 3D single object tracking (SOT) that considers each tracking sequence as a continuous stream and leverages the multi-frame motion information for more robust tracking. Our approach employs a memory-based feature extraction method to efficiently utilize multi-frame features and introduces hybrid attention to model spatial-temporal relations more effectively. We have also proposed a contrastive sequence enhancement strategy to improve the utilization of sequential information for false positive reduction. Our ex-

perimental results demonstrate that StreamTrack achieves state-of-the-art performance. We hope our work can serve as a baseline for utilizing sequential information in 3D SOT and inspire future research in this field.

References

- [1] Luca Bertinetto, Jack Valmadre, Joao F Henriques, Andrea Vedaldi, and Philip HS Torr. Fully-convolutional siamese networks for object tracking. In *European conference on computer vision*, pages 850–865. Springer, 2016. 1, 2
- [2] Holger Caesar, Varun Bankiti, Alex H Lang, Sourabh Vora, Venice Erin Liong, Qiang Xu, Anush Krishnan, Yu Pan, Giancarlo Baldan, and Oscar Beijbom. nuscenes: A multi-modal dataset for autonomous driving. In *Proceedings of the IEEE/CVF conference on computer vision and pattern recognition*, pages 11621–11631, 2020. 6
- [3] Nicolas Carion, Francisco Massa, Gabriel Synnaeve, Nicolas Usunier, Alexander Kirillov, and Sergey Zagoruyko. End-to-end object detection with transformers. In *European Conference on Computer Vision*, pages 213–229. Springer, 2020. 2
- [4] Nicolas Carion, Francisco Massa, Gabriel Synnaeve, Nicolas Usunier, Alexander Kirillov, and Sergey Zagoruyko. End-to-end object detection with transformers. In *Computer Vision—ECCV 2020: 16th European Conference, Glasgow, UK, August 23–28, 2020, Proceedings, Part I 16*, pages 213–229. Springer, 2020. 5
- [5] Ting Chen, Simon Kornblith, Mohammad Norouzi, and Geoffrey Hinton. A simple framework for contrastive learning of visual representations. In *International conference on machine learning*, pages 1597–1607. PMLR, 2020. 3, 5
- [6] Yubo Cui, Zheng Fang, Jiayao Shan, Zuoxu Gu, and Sifan Zhou. 3d object tracking with transformer. *arXiv preprint arXiv:2110.14921*, 2021. 1, 2, 6
- [7] Alexey Dosovitskiy, Lucas Beyer, Alexander Kolesnikov, Dirk Weissenborn, Xiaohua Zhai, Thomas Unterthiner, Mostafa Dehghani, Matthias Minderer, Georg Heigold, Sylvain Gelly, et al. An image is worth 16x16 words: Transformers for image recognition at scale. *arXiv preprint arXiv:2010.11929*, 2020. 2
- [8] Zheng Fang, Sifan Zhou, Yubo Cui, and Sebastian Scherer. 3d-siamrpn: An end-to-end learning method for real-time 3d single object tracking using raw point cloud. *IEEE Sensors Journal*, 21(4):4995–5011, 2020. 6
- [9] Andreas Geiger, Philip Lenz, and Raquel Urtasun. Are we ready for autonomous driving? the kitti vision benchmark suite. In *2012 IEEE conference on computer vision and pattern recognition*, pages 3354–3361. IEEE, 2012. 6
- [10] Silvio Giancola, Jesus Zarzar, and Bernard Ghanem. Leveraging shape completion for 3d siamese tracking. In *Proceedings of the IEEE/CVF Conference on Computer Vision and Pattern Recognition*, pages 1359–1368, 2019. 1, 2, 6, 7
- [11] Jean-Bastien Grill, Florian Strub, Florent Althé, Corentin Tallec, Pierre Richemond, Elena Buchatskaya, Carl Doersch, Bernardo Avila Pires, Zhaohan Guo, Mohammad Gheshlaghi Azar, et al. Bootstrap your own latent—a new approach to self-supervised learning. *Advances in neural information processing systems*, 33:21271–21284, 2020. 3
- [12] Qing Guo, Wei Feng, Ce Zhou, Rui Huang, Liang Wan, and Song Wang. Learning dynamic siamese network for visual object tracking. In *Proceedings of the IEEE international conference on computer vision*, pages 1763–1771, 2017. 1, 2
- [13] Zhiyang Guo, Yunyao Mao, Wengang Zhou, Min Wang, and Houqiang Li. Cmt: Context-matching-guided transformer for 3d tracking in point clouds. In *Computer Vision—ECCV 2022: 17th European Conference, Tel Aviv, Israel, October 23–27, 2022, Proceedings, Part XXII*, pages 95–111. Springer, 2022. 1, 2, 5, 6
- [14] Kaiming He, Haoqi Fan, Yuxin Wu, Saining Xie, and Ross Girshick. Momentum contrast for unsupervised visual representation learning. In *Proceedings of the IEEE/CVF conference on computer vision and pattern recognition*, pages 9729–9738, 2020. 3, 5
- [15] Olivier Henaff. Data-efficient image recognition with contrastive predictive coding. In *International conference on machine learning*, pages 4182–4192. PMLR, 2020. 3, 5
- [16] Le Hui, Lingpeng Wang, Mingmei Cheng, Jin Xie, and Jian Yang. 3d siamese voxel-to-bev tracker for sparse point clouds. *Advances in Neural Information Processing Systems*, 34, 2021. 1, 2, 6
- [17] Le Hui, Lingpeng Wang, Linghua Tang, Kaihao Lan, Jin Xie, and Jian Yang. 3d siamese transformer network for single object tracking on point clouds. In *Computer Vision—ECCV 2022: 17th European Conference, Tel Aviv, Israel, October 23–27, 2022, Proceedings, Part II*, pages 293–310. Springer, 2022. 1, 2, 5, 6, 8
- [18] Matej Kristan, Jiri Matas, Aleš Leonardis, Tomáš Vojtíš, Roman Pflugfelder, Gustavo Fernandez, Georg Nebelhay, Fatih Porikli, and Luka Čehovin. A novel performance evaluation methodology for single-target trackers. *IEEE transactions on pattern analysis and machine intelligence*, 38(11):2137–2155, 2016. 6
- [19] Christopher Lang, Alexander Braun, and Abhinav Valada. Contrastive object detection using knowledge graph embeddings. *arXiv preprint arXiv:2112.11366*, 2021. 3
- [20] Bo Li, Wei Wu, Qiang Wang, Fangyi Zhang, Junliang Xing, and Junjie Yan. Siamrpn++: Evolution of siamese visual tracking with very deep networks. In *Proceedings of the IEEE/CVF Conference on Computer Vision and Pattern Recognition*, pages 4282–4291, 2019. 1, 2
- [21] Bo Li, Junjie Yan, Wei Wu, Zheng Zhu, and Xiaolin Hu. High performance visual tracking with siamese region proposal network. In *Proceedings of the IEEE conference on computer vision and pattern recognition*, pages 8971–8980, 2018. 1, 2
- [22] Feng Li, Hao Zhang, Shilong Liu, Jian Guo, Lionel M Ni, and Lei Zhang. Dn-detr: Accelerate detr training by introducing query denoising. In *Proceedings of the IEEE/CVF Conference on Computer Vision and Pattern Recognition*, pages 13619–13627, 2022. 5
- [23] Tsung-Yi Lin, Priya Goyal, Ross Girshick, Kaiming He, and Piotr Dollár. Focal loss for dense object detection. In *Pro-*

- ceedings of the IEEE international conference on computer vision, pages 2980–2988, 2017. 5
- [24] Ze Liu, Yutong Lin, Yue Cao, Han Hu, Yixuan Wei, Zheng Zhang, Stephen Lin, and Baining Guo. Swin transformer: Hierarchical vision transformer using shifted windows. In *Proceedings of the IEEE/CVF international conference on computer vision*, pages 10012–10022, 2021. 2
- [25] Aaron van den Oord, Yazhe Li, and Oriol Vinyals. Representation learning with contrastive predictive coding. *arXiv preprint arXiv:1807.03748*, 2018. 3, 5
- [26] Charles R Qi, Or Litany, Kaiming He, and Leonidas J Guibas. Deep hough voting for 3d object detection in point clouds. In *Proceedings of the IEEE/CVF International Conference on Computer Vision*, pages 9277–9286, 2019. 2
- [27] Charles R Qi, Li Yi, Hao Su, and Leonidas J Guibas. Pointnet++: Deep hierarchical feature learning on point sets in a metric space. *arXiv preprint arXiv:1706.02413*, 2017. 3, 4
- [28] Haozhe Qi, Chen Feng, Zhiguo Cao, Feng Zhao, and Yang Xiao. P2b: Point-to-box network for 3d object tracking in point clouds. In *Proceedings of the IEEE/CVF Conference on Computer Vision and Pattern Recognition*, pages 6329–6338, 2020. 1, 2, 3, 5, 6, 7, 8
- [29] Hamid Rezaatoughi, Nathan Tsoi, JunYoung Gwak, Amir Sadeghian, Ian Reid, and Silvio Savarese. Generalized intersection over union: A metric and a loss for bounding box regression. In *Proceedings of the IEEE/CVF conference on computer vision and pattern recognition*, pages 658–666, 2019. 5
- [30] Jiayao Shan, Sifan Zhou, Zheng Fang, and Yubo Cui. Ptt: Point-track-transformer module for 3d single object tracking in point clouds. In *2021 IEEE/RSJ International Conference on Intelligent Robots and Systems (IROS)*, pages 1310–1316. IEEE, 2021. 2, 6
- [31] Shaoshuai Shi, Xiaogang Wang, and Hongsheng Li. Pointcnn: 3d object proposal generation and detection from point cloud. In *Proceedings of the IEEE/CVF conference on computer vision and pattern recognition*, pages 770–779, 2019. 5
- [32] Pei Sun, Henrik Kretschmar, Xerxes Dotiwalla, Aurelien Chouard, Vijaysai Patnaik, Paul Tsui, James Guo, Yin Zhou, Yuning Chai, Benjamin Caine, et al. Scalability in perception for autonomous driving: Waymo open dataset. In *Proceedings of the IEEE/CVF Conference on Computer Vision and Pattern Recognition*, pages 2446–2454, 2020. 6
- [33] Ran Tao, Efstratios Gavves, and Arnold WM Smeulders. Siamese instance search for tracking. In *Proceedings of the IEEE conference on computer vision and pattern recognition*, pages 1420–1429, 2016. 1, 2
- [34] Hugues Thomas, Charles R Qi, Jean-Emmanuel Deschaud, Beatriz Marcotegui, François Goulette, and Leonidas J Guibas. Kpconv: Flexible and deformable convolution for point clouds. In *Proceedings of the IEEE/CVF international conference on computer vision*, pages 6411–6420, 2019. 4
- [35] Ashish Vaswani, Noam Shazeer, Niki Parmar, Jakob Uszkoreit, Llion Jones, Aidan N Gomez, Łukasz Kaiser, and Illia Polosukhin. Attention is all you need. In *Advances in neural information processing systems*, pages 5998–6008, 2017. 2, 3, 4
- [36] Yue Wang, Yongbin Sun, Ziwei Liu, Sanjay E Sarma, Michael M Bronstein, and Justin M Solomon. Dynamic graph cnn for learning on point clouds. *Acm Transactions On Graphics (tog)*, 38(5):1–12, 2019. 4
- [37] Zhoutao Wang, Qian Xie, Yu-Kun Lai, Jing Wu, Kun Long, and Jun Wang. Mlvsnet: Multi-level voting siamese network for 3d visual tracking. In *Proceedings of the IEEE/CVF International Conference on Computer Vision*, pages 3101–3110, 2021. 1, 2, 6
- [38] Junfeng Wu, Qihao Liu, Yi Jiang, Song Bai, Alan Yuille, and Xiang Bai. In defense of online models for video instance segmentation. In *Computer Vision–ECCV 2022: 17th European Conference, Tel Aviv, Israel, October 23–27, 2022, Proceedings, Part XXVIII*, pages 588–605. Springer, 2022. 3
- [39] Zhirong Wu, Yuanjun Xiong, Stella X Yu, and Dahua Lin. Unsupervised feature learning via non-parametric instance discrimination. In *Proceedings of the IEEE conference on computer vision and pattern recognition*, pages 3733–3742, 2018. 3, 6
- [40] Lewei Yao, Renjie Pi, Hang Xu, Wei Zhang, Zhenguo Li, and Tong Zhang. G-detkd: towards general distillation framework for object detectors via contrastive and semantic-guided feature imitation. In *Proceedings of the IEEE/CVF international conference on computer vision*, pages 3591–3600, 2021. 3
- [41] Hengshuang Zhao, Li Jiang, Jiaya Jia, Philip HS Torr, and Vladlen Koltun. Point transformer. In *Proceedings of the IEEE/CVF International Conference on Computer Vision*, pages 16259–16268, 2021. 4
- [42] Chaoda Zheng, Xu Yan, Jiantao Gao, Weibing Zhao, Wei Zhang, Zhen Li, and Shuguang Cui. Box-aware feature enhancement for single object tracking on point clouds. In *Proceedings of the IEEE/CVF International Conference on Computer Vision*, pages 13199–13208, 2021. 1, 2, 3, 4, 5, 6, 7, 8
- [43] Chaoda Zheng, Xu Yan, Haiming Zhang, Baoyuan Wang, Shenghui Cheng, Shuguang Cui, and Zhen Li. Beyond 3d siamese tracking: A motion-centric paradigm for 3d single object tracking in point clouds. In *Proceedings of the IEEE/CVF Conference on Computer Vision and Pattern Recognition*, pages 8111–8120, 2022. 1, 2, 3, 4, 5, 6, 7, 8
- [44] Changqing Zhou, Zhipeng Luo, Yueru Luo, Tianrui Liu, Liang Pan, Zhongang Cai, Haiyu Zhao, and Shijian Lu. Pptr: Relational 3d point cloud object tracking with transformer. In *Proceedings of the IEEE/CVF Conference on Computer Vision and Pattern Recognition*, pages 8531–8540, 2022. 1, 2, 3, 5, 6
- [45] Xiaoyu Zhou, Ling Wang, Zhian Yuan, Ke Xu, and Yanxin Ma. Structure aware 3d single object tracking of point cloud. *Journal of Electronic Imaging*, 30(4):043010, 2021. 2, 6
- [46] Benjin Zhu, Zhe Wang, Shaoshuai Shi, Hang Xu, Lanqing Hong, and Hongsheng Li. Conquer: Query contrast voxel-detr for 3d object detection. *arXiv preprint arXiv:2212.07289*, 2022. 3